学位論文

Selective dysregulation of Epstein-Barr virus infection in hypomorphic *ZAP70* mutation

（部分的機能低下型 *ZAP70* 変異は EB ウイルスに対して選択的な免疫応答の異常をきたす）

医学薬学教育部博士課程

生命・臨床医学専攻

学籍番号　31261017

星野　顕宏

Abstract of the thesis

Background. Some types of genetic defects develop Epstein-Barr virus (EBV)-associated lymphoproliferative disorder (LPD)/lymphoma as the main feature. Hypomophic mutations can cause different clinical and laboratory manifestations from null mutations in the same genes.

Methods. We sought to describe the clinical and immunologic phenotype of a 21-month-old boy having EBV-associated LPD who was in good health till then. A genetic and immunologic analysis was performed.

Results. Whole exome sequencing identified a novel compound heterozygous mutation of *ZAP70* c.703-1G>A and c.1674G>A. A small amount of the normal transcript was observed. Unlike ZAP70 deficiency which is previously described as severe combined immunodeficiency with non-functional $CD4^+$ T cells and absent $CD8^+$ T cells, the patient had slightly low numbers of $CD8^+$ T cells and a small amount of functional T cells. EBV-specific $CD8^+$ T cells and invariant NKT (iNKT) cells were absent. The T-cell receptor repertoire using next generation sequencing was significantly restricted and the patient had no EBV specific *TRBV* complementarity determining region 3 sequence.

Conclusions. Our patient shows that a hypomorphic mutation of *ZAP70* can lead to EBV-associated LPD and that EBV-specific $CD8^+$ T cells and iNKT cells are critically involved in immune response against EBV infection.

CONTENTS

LIST OF FIGURES AND TABLES

INTRODUCTION

Epstein-Barr virus (EBV) infects the majority of population worldwide. Primary EBV infection is asymptomatic or occasionally causes infectious mononucleosis. Following primary infection, although EBV is not eliminated in memory B cells for the lifetime of the hosts, EBV is latently maintained being controlled by the host immune response [1]. In this setting, EBV-specific T cells play important roles [1-3]. Indeed, in human immunodeficiency virus-infected or post-transplant patients, impaired T-cell response allows EBV-infected cells to become proliferating blasts, which can result in lymphoproliferative disease (LPD) or lymphoma [4, 5]. Although humanized mouse models have partially contributed to reveal immune response against EBV infection [6], the details remain unclear. Some types of genetic defects are known and recently described for developing EBV-associated LPD/lymphoma as the main feature [7-11]. These disorders include signaling lymphocytic activation molecule-associated protein (SAP) deficiency [7, 8], interleukin-2 inducible T-cell kinase (ITK) deficiency [9], CD27 deficiency [10], X-linked immunodeficiency with magnesium defect, EBV infection, and neoplasia (XMEN) disease [11] (Intro Figure A). These primary immunodeficiencies (PIDs) provided new insights of roles of T-cell receptor (TCR) or associated co-stimulatory signals and added evidences of critically involvement of invariant natural killer T (iNKT) cells in immune response against EBV infection [2, 3].

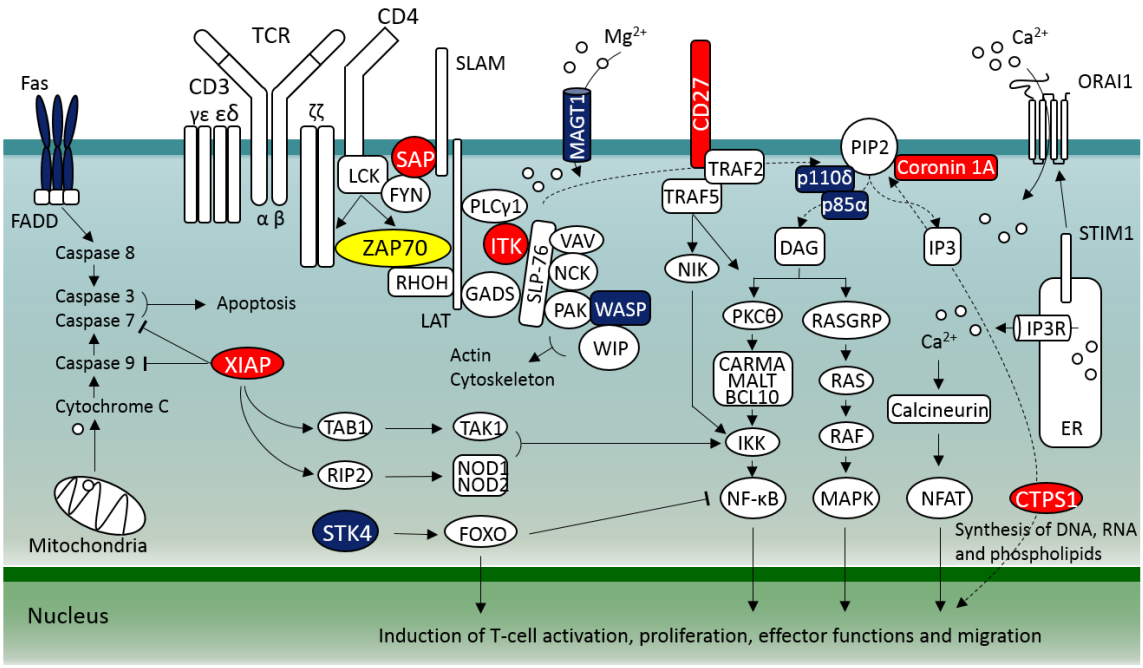

Intro Figure A. T-cell receptor (TCR) and associated co-stimulatory signals (modified from reference 2). Mutant molecules in patients with EBV susceptibility are indicated in blue and those without invariant NKT cell are indicated in red. After TCR stimulation, ZAP70 (yellow) is recruited to the CD3ζ chain and phosphorylated by LCK, which results in activation of ZAP70 catalytic activity. Active ZAP70 subsequently phosphorylates LAT and SLP-76, which function as scaffolds to recruit many other signaling molecules and lead to T-cell activation, proliferation, effector functions and migration. BCL10, B-cell lymphoma/leukaemia 10; CARMA, CARD-containing MAGUK protein; CTPS1, cytidine 5' triphosphate synthase 1; DAG, diacylglycerol; ER, endoplasmic reticulum; FADD: Fas-associated protein with death domain; FOXO, forkhead box O; GADS, Grb2-related adaptor downstream of Shc; IKK, IkB kinase; IP3, inositol trisphosphate; IP3R, inositol trisphosphate receptor; ITK, interleukin-2 inducible T-cell kinase; LAT: linker for activation of T cells; LCK: lymphocyte-specific protein tyrosine kinase; MAGT1, magnesium transporter 1; MALT, mucosa-associated lymphoid tissue lymphoma

translocation protein; MAPK, mitogen-activated protein kinase; NCK, non-catalytic region of tyrosine kinase adaptor protein; NFAT, nuclear factor of activated T cells; NF-κB, nuclear factor-κB; NIK, NF-κB-inducing kinase; NOD, nucleotide-binding oligomerization domain; PIP2, phosphatidyl inositol bisphosphate; PKCθ, protein kinase C θ; PLCγ1, phospholipase Cγ1; RASGRP, Ras guanyl nucleotide-releasing protein; RHOH, Ras homolog gene family member H; RIP2, receptor-interacting serine/threonine protein kinase 2; SAP, SLAM-associated protein; SLAM, signalling lymphocyte activation molecule; SLP-76, SH2 domain-containing leucocyte protein of 76 kd; STIM1, stromal interaction molecule 1; STK4, serine/threonine protein kinase 4; TAB1, TAK1-binding protein; TAK1, transforming growth factor-beta-activated kinase 1; TRAF, tumor necrosis factor receptor associated factor; WASP, Wiskott-Aldrich syndrome protein; WIP, WASP-interacting protein; XIAP, X-linked inhibitor of apoptosis protein; ZAP70, zeta-chain associated protein kinase, 70 kd.

Intro Table A. Primary immunodeficiencies predominantly presenting with EBV-associated diseases (modified from reference 2).

Genetic disorder	Inheritance	Gene	HLH	Chronic EBV viremia	Lymphoma	Dysgammaglobulin-emia	iNKT cell count
SAP deficiency	XL	*SH2D1A*	+	-	+	+	↓
XIAP deficiency	XL	*XIAP*	+	-	-	+	NL/↓
ITK deficiency	AR	*ITK*	+	+	+	+	↓
CD27 deficiency	AR	*CD27*	+	+	+	+	NL/↓
XMEN disease	XL	*MAGT1*	-	+	+	+	NL
STK4 deficiency	AR	*STK4*	-	+	+	+	?
Coronin 1A deficiency	AR	*CORO1A*	-	+	+	+	↓
APDS	AD	*PIK3CD*	+	+	+	+	NL
CTPS1 deficiency	AR	*CTPS1*	-	+	+	-	↓
ALPS-FAS	AD	*FAS*	+	+	+	+	?
ZAP70 deficiency*	AR	*ZAP70*	-	+	+	+	-

AD, autosomal dominant; ALPS, autoimmune lymphoproliferative syndrome; APDS, activated PI3Kδ syndrome; AR, autosomal recessive; CTPS1, cytidine 5' triphosphate synthase 1; EBV, Epstein-Barr virus; HLH, hemophagocytic lymphohistiocytosis; iNKT, invariant natural killer; ITK, interleukin-2 inducible T-cell kinase; NL, normal; SAP, SLAM-associated protein; STIM1, stromal interaction molecule 1; STK4, serine/threonine protein kinase 4; XIAP, X-linked inhibitor of apoptosis protein; XL, X-linked; XMEN, X-linked immunodeficiency with magnesium defect, EBV infection, and neoplasia; ZAP70, zeta-chain associated protein kinase, 70 kd.

* Novel findings in this report.

Here we describe an EBV-LPD patient associated with a hypomorphic mutation of *zeta-chain associated protein kinase, 70 kd* (*ZAP70*), who showed pivotal roles of T-cell recognition and iNKT cells in the control of EBV. ZAP70 is a non-receptor tyrosine kinase which is a key component of the TCR signal transduction pathway [12, 13] (Intro Figure A). ZAP deficiency is previously described as severe combined immunodeficiency (SCID) with non-functional $CD4^+$ T cells and absent $CD8^+$ T cells [14]. The patient was in good health until EBV infection with a few functional $CD4^+$ and $CD8^+$ T cells. However, selective dysregulation of EBV infection was revealed by cytomolecular analysis including TCR repertoire analysis using next generation sequencing (NGS).

MATREIALS AND METHODS

Ethical Considerations

The informed consent was obtained from the patient's parents. The study was conducted in accordance with the Helsinki Declaration and was approved by the ethics board of the University of Toyama and Tokyo Medical and Dental University.

Genetic Analysis (See supplementary Figure 1 [15])

Whole exome sequencing (WES) was performed using genomic DNA from whole blood of the patient and his parents [16]. Exome capture was carried out using a SureSelect Human All Exon V5 kit (Agilent technologies, Santa Clara, CA), and massively-parallel sequencing was performed using a HiSeq 2000 platform (Illumina, San Diego, CA) with 100 bp-paired-end reads. The data were processed with an in-house constructed analysis pipeline, which conducted the

alignment of the reads with Burrows-Wheeler aligner 0.5.8 [17], counting of variant allele numbers with Samtools [18], and annotation with ANNOVAR [19]. Identified variants were filtered using dbSNP131, an in-house SNP database, and the Human Genetic Variation Database (http://www.genome.med.kyoto-u.ac.jp/SnpDB/). Predicted functional effects of variants were determined using SIFT [20], PhyloP [21], PolyPhen2 [22], and MutationTaster [23]. In order to validate the results, polymerase chain reaction (PCR) using primers listed in Supplementary Table 1 and capillary sequencing was performed.

RT-PCR and Detection of Splicing Product

RNA was extracted from peripheral blood mononuclear cells (PBMCs) according to standard methods and cDNA was prepared using SuperScript VILO (Invitrogen, Carlsbad, CA). PCR was performed using cDNA. The PCR products were cloned using TOPO TA cloning kit (Life Technologies, Carlsbad, CA) and independent clones were sequenced. Primers were listed in Supplementary Table 1.

Flow Cytometry

PBMCs were stained with fluorochrome-conjugated antibodies. Stained cells were analyzed using BD LSRFortessa (BD Biosciences, San Jose, CA) and the data processed using FlowJo software (Tree Star Inc., Ashland, OR). For lymphocyte phenotyping, monoclonal antibodies used to stain cell surface were listed in Supplementary Table 2. For EBV-specific $CD8^+$ T cells, PBMCs were incubated with Clear Back (MBL, Nagoya, Japan) to block the Fc receptors, and stained with HLA-A*24:02 EBV mix Tetramer-phycoerythrin (PE) (MBL), followed by PE-Vio770-conjugated anti-CD8 (clone BW135/80, Miltenyi Biotec, Germany). For intracellular

ZAP70 staining, PBMCs were labeled with VioGreen-conjugated anti-CD3 (clone BW264/56, Miltenyi Biotec), VioBlue-conjugated anti-CD4 (clone M-T466, Miltenyi Biotec) and PE-Vio770-conjugated anti-CD8. Then, cells were fixed and permeabilized with Fixation/Permeabilization kit (eBioscience, San Diego, CA), washed in permeabilization buffer (eBioscience) and stained with PE-conjugated anti-ZAP70 (clone 1E7.2, eBioscience).

Functional Analysis

For calcium flux analysis, PBMCs were loaded with 2 μM Fluo-4 AM (Life Technologies) for 45 min at 37 °C and stained for CD4 and CD8. Cells were stimulated with mouse anti-human CD3 (1 μg/ml; clone UCHT1, BD Pharmingen, San Diego, CA) and goat anti-mouse antibodies (BD Pharmingen), or ionomycin (8 μg/ml; Life technologies). The analysis was performed by flow cytometry and kinetic plots using FlowJo software. For T-cell proliferation analysis, PBMCs were labeled with CFSE (3 μM; eBioscience) for 5 min at room temperature and stimulated for 4 days with anti-CD3/CD28 activating Dynabeads (Life Technologies, Oslo, Norway), or phorbol myristate acetate (PMA, 10 ng/mL; Sigma-Aldrich) and ionomycin (0.25 μg/mL; Sigma-Aldrich). Then, cells were stained for CD4 and CD8, and analyzed by flow cytometry.

TCR Repertoire Analysis (See supplementary Figure 2 [24])

cDNA from PBMCs was amplified using the HTBI-M reagent system (iRepertoire Inc., Huntsville, AL) according to the manufacturer's protocol, which include nested primers targeting each of the V and J elements for the first round of PCR and communal primers for the second round of PCR. After gel purification, the resulting product were sequenced using a MiSeq

platform (Illumina). The data were processed with a provided pipeline (iRepertoire Inc.). For each sequence, copy number, complementarity determining region 3 (CDR3) length, V and J usage, N addition and V and J trimming were determined. Shannon entropy was calculated [25].

T-cell receptor excision circles (TRECs) Analysis (See supplementary Figure 3 [26])

TRECs quantification was performed using DNA from whole blood. Real-time PCR for δRec-ψJα TRECs was performed with primers which span TRECs and probe using LightMix Modular TREC (Roche Diagnostics, Indianapolis, IN). As an internal control, MSTN gene was amplified using LightMix Modular MSTN Extraction Control (Roche Diagnostics) [27].

Quantitation of DNA Copy Number (See supplementary Figure 4)

In order to determine the ratio of X and Y chromosome, the copy number of *IL2RG* and *SRY*, which are on X and Y chromosome, respectively, were measured. Droplet digital PCR (ddPCR) was performed using QX200 Droplet Digital PCR System (Bio-Rad Laboratories, Hercules, CA) [28]. The primers and the hydrolysis probes were listed in Supplementary Table 3. The *IL2RG* probes were labeled with HEX and *SRY* probe was labeled with FAM.

Immunohistochemical Staining

Pathological analysis was performed on cervical lymph node tissue. For immunohistochemistry, antibodies against cytoplasmic CD3, CD4, CD8, CD20 (Nichirei Biosciences, Tokyo, Japan), latent membrane protein 1 (LMP1, clone CS.1-4, DAKO, Tokyo, Japan), Epstein-Barr virus nuclear 2 (EBNA2, clone PE2, DAKO) were used. EBV genome was detected by *in situ* hybridization using EBV-encoded RNA signals (EBERs, EBER PNA probe, DAKO).

RESULTS

Clinical Features

A 21-month-old boy presented with fever, systemic lymphadenopathy and facial paralysis. The patient was found to have enlarged spleen and EBV viremia (24,000 copies/10^6 cells). He was born to nonconsanguineous Japanese parents, and was in good health until he was admitted. He was immunized with live measles-rubella and BCG without adverse effect. His parents and 3 elder siblings were healthy except for the second brother. The brother died of acute encephalopathy at the age of 6 years, and his $CD8^+$ T-cell counts were within normal range. The patient was diagnosed with EBV-associated LPD, as described below. The patient temporarily responded to corticosteroid, however, he developed mass lesions in his brain, liver, kidneys and lungs when he was 24 months old. They were refractory to the therapy including anti-CD20 antibodies and chemotherapy. Subsequently the mass lesion also appeared in his heart, which led to his death due to fetal atrioventricular block at 27 months of age.

Pathological Findings

Figure 1 shows histologic findings of the cervical lymph node before chemotherapy. Normal architecture of the lymph node was partially effaced and large and medium-sized lymphoid cell proliferation was observed. Large lymphoid cells were positive for CD20 and EBERs, while medium-sized lymphoid cells were positive for cytoplasmic CD3 and CD8 or CD4. Staining with EBNA2 and LMP1was positive, which indicated type III latency pattern.

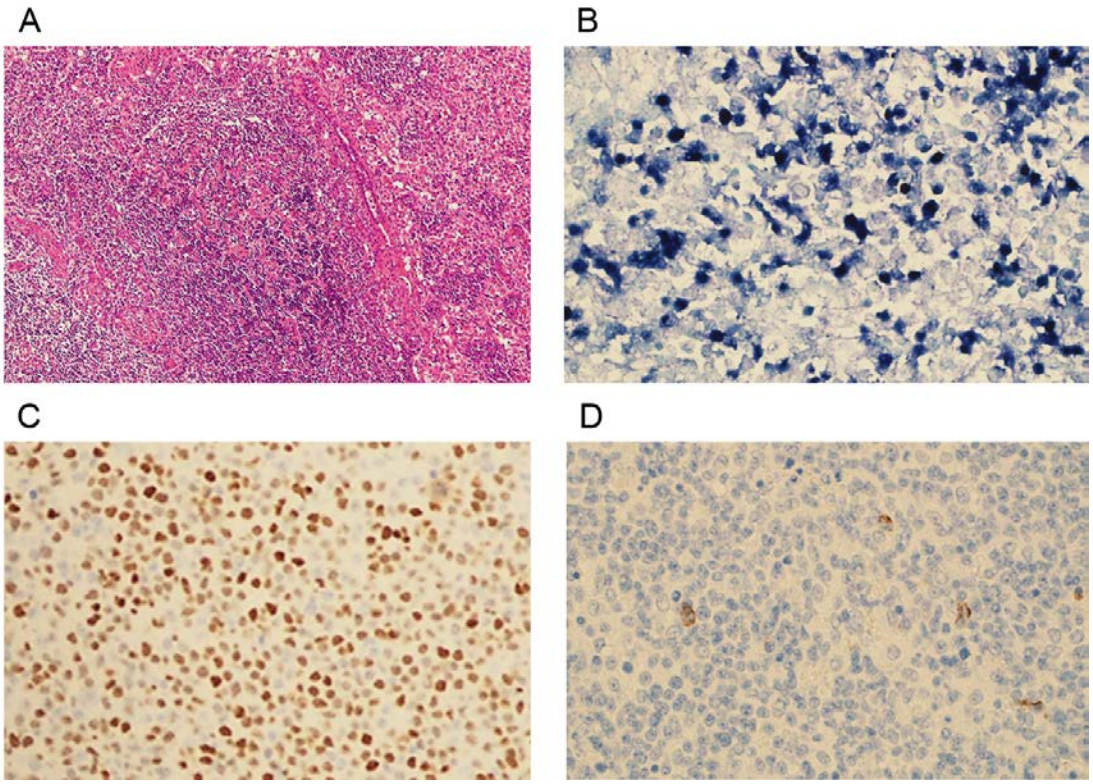

Figure 1. Pathological findings of the lymph node. (A) Normal architecture of the cervical lymph node is partially effaced and large and medium-sized lymphoid cell proliferation is observed (hematoxylin-eosin stain, 100×). (B, C) Most of large lymphoid cells were positive for EBER (B, 400×) and EBNA2 (C, 400×). (D) Few large lymphoid cells were positive for LMP1 (400×).

Immunodeficiency

The immunological data are summarized in Table 1. Total lymphocyte counts were normal, but T-cell counts were low with decreased, but not absent, $CD8^+$ T-cell counts (5%). Interestingly, $CD8^+$ T-cell percentages were increased to 12% in total lymphocytes with 1.2 of CD4/CD8 ratio, when the patient was 24 months old. B- and NK-cell counts were almost within normal range. Before intravenous immunoglobulin, serum IgG, IgA and IgM levels were elevated. He had

protective titers of measles and rubella antibodies as postvaccination titers; however, antibodies for EBV viral capsid antigen (VCA) IgG, VCA IgM and EBNA antibodies were negative 3 weeks after onset of symptoms.

Table 1. Immunophenotyping of the patient

		before treatmnt (21 montehs)	3 months after last chemotherapy (24 months)	Normal values†
Lymphocytes, /μL		4480	640	3600-8900
T cells, % (/μL)	$CD3^+$/Lym	34 (1520)	35 (220)	59-72 (2100-6400)
Helper T cells, % (/μL)	$CD4^+$/Lym	27 (1210)	14 (88)	38-54 (1400-4800)
Naïve $CD4^+$ T cells, %	$CD45RA^+/CD3^+CD4^+$	ND	4	77-89
Memory $CD4^+$ T cells, %	$CD45RO^+/CD3^+CD4^+$	ND	95	11-23
Recent thymic emigrants, %	$CD31^+/CD3^+CD4^+CD45RA^+$	ND	31	84-96
T follicular helper cells, %	$CD45RO^+CXCR5^+/CD3^+CD4^+$	ND	3	1-4
Regulatory T cells, %	$CD25^+CD127^-/CD3^+CD4^+CCR4^+$	ND	13	15-31
Cytotoxic T cells, % (/μL)	$CD8^+$/Lym	5 (220)	12 (74)	7-23 (390-2000)
Naïve $CD8^+$ T cells, %	$CD45RA^+/CD3^+CD8^+$	ND	4	78-91
Memory $CD8^+$ T cells, %	$CD45RO^+/CD3^+CD8^+$	ND	96	9-22
Central memory T cells, %	$CD62L^+CCR7^+/CD3^+CD8^+CD45RO^+$	ND	4	37-62
Effector memory T cells, %	$CD62L^-CCR7^-/CD3^+CD8^+CD45RO^+$	ND	61	10-30
TCRδγ T cells, %	$TCR\alpha\beta^-TCR\gamma\delta^+/CD3^+$	ND	20	1-13
Double negative T cells, %	$CD4^-CD8^-/CD3^+TCR\alpha\beta^+$	ND	21	1-2
invariant NKT cells, %	TCR $V\alpha24^+$TCR $V\beta11^+/CD3^+$	ND	0.00	0.01-0.12
B cells, % (/μL)	$CD19^+CD20^+$/Lym	36 (1610)	2 (14)*	8-22 (470-2000)
NK cells, % (/μL)	$CD16^+CD56^+$/Lym	27 (1210)	39 (250)	1-10 (100-1000)
IgG, g/L		16.01		5.53-9.71‡
IgA, g/L		1.82		0.26-0.74‡
IgM, g/L		2.82		0.35-0.81‡
Measles IgG, IU/mL		2200 (protective)		
Rubella IgG, IU/mL		93.0 (protective)		
EBV VCA IgM		<10		
EBV VCA IgG		<10		
EBNA antibodies		<10		
TRECs, copies/μg DNA		Negative		$3.5\text{-}8.1 \times 10^3$§

ND, not determined; TCR, T-cell receptor; NKT, natural killer T; EBV, Epstein-Barr virus; VCA, viral capsid antigen; EBNA, Epstein-Barr nuclear antigen; TRECs, T-cell receptor excision circles.

* 3 months after last anti-CD20 antibodies.

† Age-matched normal values in Japanese as established by the performing laboratory.

‡ Reference 29.

§ Reference 27.

The immunophenotypic analysis of T-cell subpopulations revealed markedly decreased proportions of both naïve $CD4^+$ and $CD8^+$ T cells. We also found increased TCRγδ T-cell and double negative T-cell counts, and decreased iNKT cell counts, suggesting aberrant development of T cells. Especially, iNKT cells were near to absent (Figure 2A). EBV-specific $CD8^+$ T-cell counts were severely diminished (Figure 2B), consisting with the histologic findings with latency type III [30]. It should be noted that these data were obtained 3 months after last chemotherapy and anti-CD20 antibodies. In order to evaluate the influence of the chemotherapy, we measured iNKT-cell counts in subjects during or after chemotherapy and/or anti-CD20 antibodies, which were not different from those in healthy control subjects (Figure 2C). These findings suggest that lack of iNKT cells is not due to chemotherapy, but due to underlying disease. TRECs levels were negative.

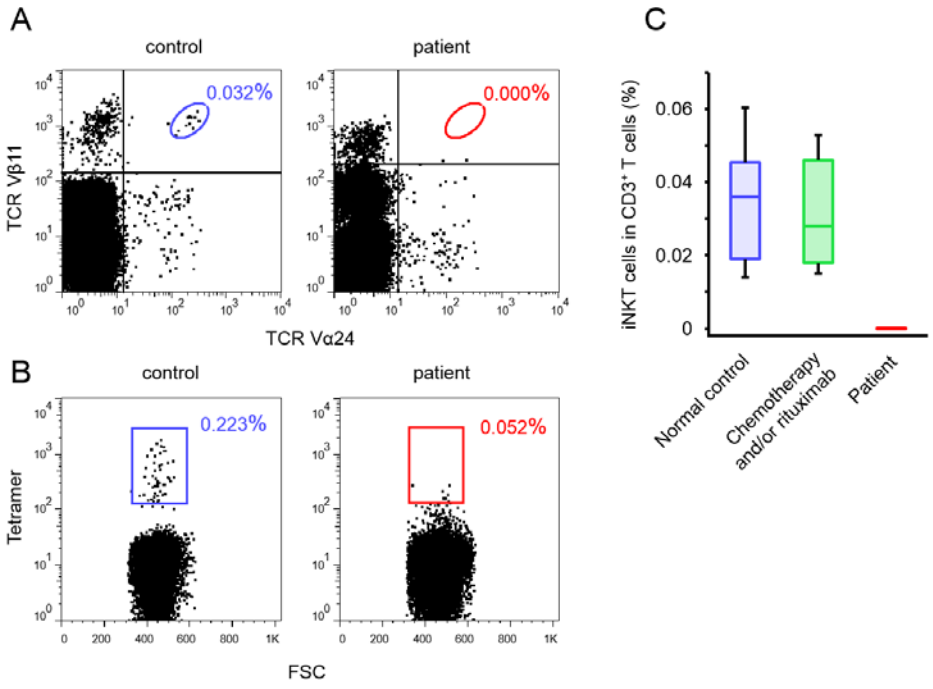

Figure 2. iNKT cells and EBV-specific $CD8^+$ T cells. (A) TCR $V\alpha24^+$ $V\beta11^+$ iNKT cells gated on $CD3^+$ T cells (left, healthy control subject; right, patient). (B) HLA-A*24:02 EBV mix $Tetramer^+$ EBV-specific cells gated on $CD8^+$ T cells (left, healthy control subject; right, patient). (C) iNKT-cell counts in healthy control subjects (n = 11), subjects during or after chemotherapy and/or anti-CD20 antibodies (n = 4), and the patient.

Identification of *ZAP70* Mutation

The immunological data suggested that the patient have a specific susceptibility to EBV. We hypothesized that this susceptibility was caused by a single gene disorder, and performed WES using DNA samples from the patient and his parents. As a result of filtering called variants (Table 2), 5 candidate variants were identified including novel 2 variants which are compound heterozygous *ZAP70* mutation c.703-1G>A and c.1674G>A (p.Met558Ile) (Table 3). The other 3 variants were not considered as disease causing genes because of the following reasons. First, the genes were not related to immune system. Second, the variants were not inactivating mutations. Third, the variants were not predicted as damaging using functional prediction algorithms.

Table 2. Filtering and numbers of called variants

Filtering step	Number of variants
Total variants in the patient	43728
Nonsynonymous variants	26812
dbSNP131-based filtering	16693
In-house SNP database-based filtering	6071
Ranking by allele frequency*	374
Inheritance model filtering	15†
HGVD-based filtering	5

SNP, Single nucleotide polymorphism; HGVD, Human Genetic Variation Database.

* Exclude variants having allele frequencies of less than 0.25 (SNVs) or 0.10 (indels).

† Homozygous, 3; compound heterozygous, 8; and de novo, 4.

Table 3. Candidate variants detected by whole exome sequence

Gene	Effect	CDS change	Protein change	Genotype	Chromosome
ZAP70	missense	c.1674G>A	p.Met558Ile	hetero	2q
ZAP70	splice site	c.703-1G>A	splice variant	hetero	2q
VOPP1	missense	c.51G>C	p.Leu17Phe	hetero	7p
PTGS1	missense	c.571C>T	p.Arg191Cys	hetero	9q
PIF1	missense	c.302T>C	p.Val101Ala	hetero	15q

CDS, coding sequence

We confirmed the compound heterozygous *ZAP70* mutations by Sanger sequencing (Figure 3A, B and C). The c.703-1G>A mutation was present in his father and the c.1674G>A mutation was present in his mother (Figure 3B). Sequencing of RT-PCR product from RNA sample revealed a splice variant lacking exon 6 (Figure 3D). Exon 6 includes binding site to CD3 immunoreceptor tyrosine-based activation motifs (Figure 3E), and Met558 is highly conserved (Figure 3F). These findings suggest the compound heterozygous *ZAP70* mutations c.703-1G>A and c.1674G>A are disease causing.

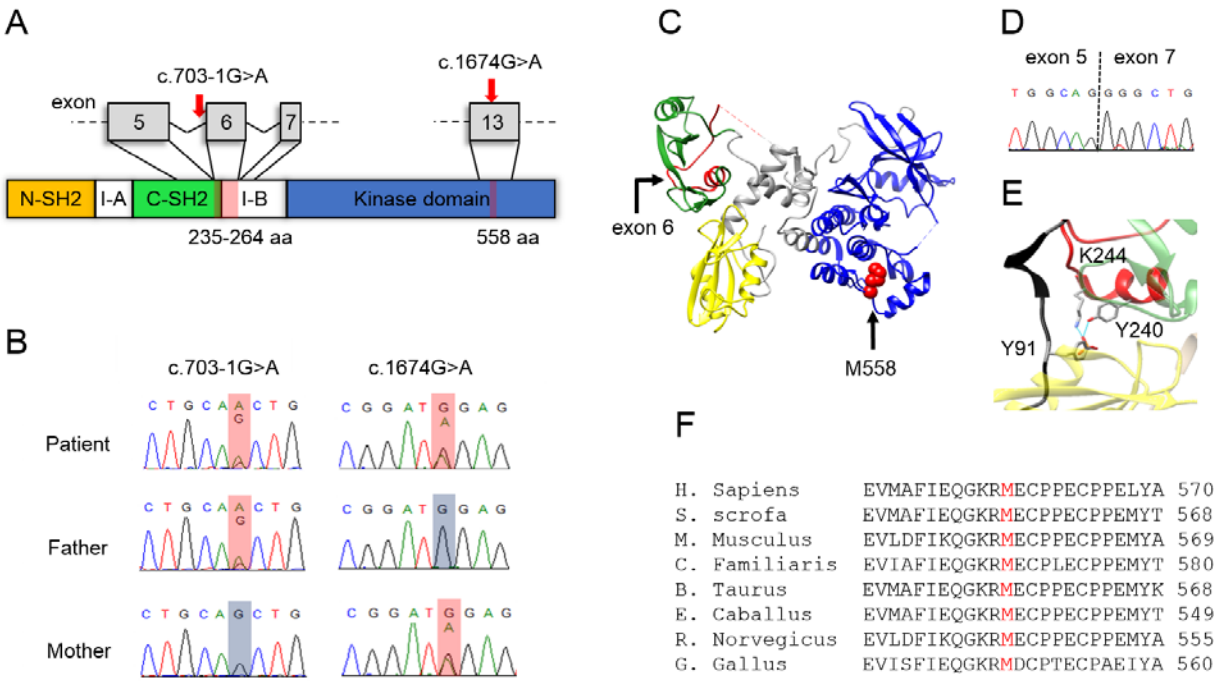

Figure 3. Genetic analysis of compound heterozygous mutation of *ZAP70*. (A) Schematic ZAP70 with N-SH2 domain (yellow), C-SH2 domain (green) and kinase domain (blue). The position of exon 6 and M558 is shown in red. Red arrows point c.703-1G>A and c.1674G>A variants. (B) Sanger sequencing of the family. Wild type c.703-1 or c.1674 positions are highlighted in blue. Heterozygous c.703-1G>A or c.1674G>A variants were highlighted in red. (C) Cristal structure of autoinhibited ZAP70 (Protein Data Bank 2OZO) produced using Chimera [31]. Affected lesions are shown in red. (D) RT-PCR reveals a splice variant lacking exon 6. (E) Cristal structure of ZAP70 and CD3 immunoreceptor tyrosine-based activation motifs (black) (Protein Data Bank 2OQ1). ZAP70 Y240 and K244 are essential to bind CD3. (F) Multiple sequence alignment of ZAP70 from different species. M558 is highly conserved.

Reduced Expression of ZAP70 Protein

ZAP70 protein expression in T cells was analyzed using flow cytometry. ZAP70 expression was reduced in $CD4^+$ and $CD8^+$ T cells from the patient (Figure 4). There is no difference in ZAP70 expression between $CD4^+$ and $CD8^+$ T cells in the patient.

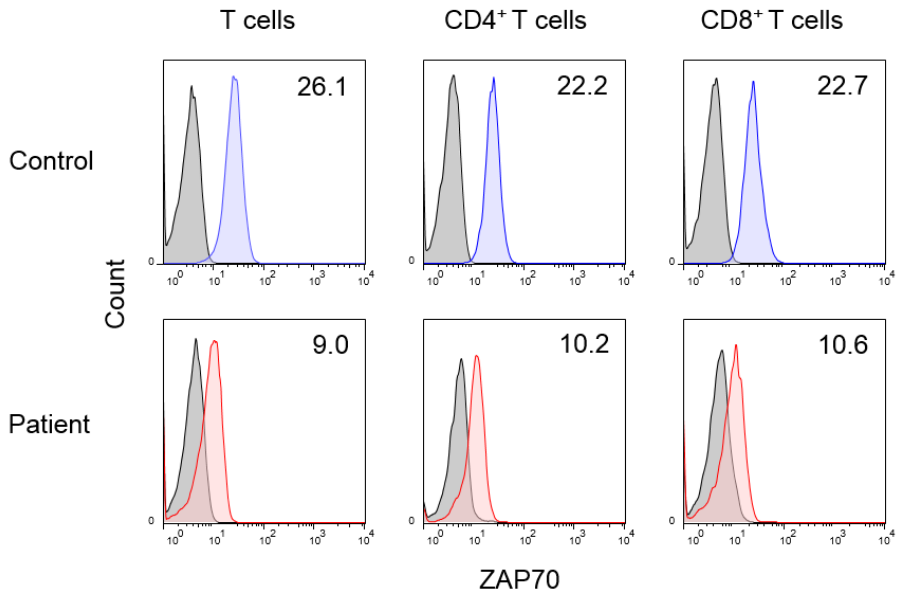

Figure 4. Expression of ZAP70. Flow cytometric analysis of ZAP70 expression in T cells, $CD4^+$ T cells and $CD8^+$ T cells (blue, control; red, patient). Numbers in plots indicate the difference in mean fluorescence intensity.

Detection of Wild Type Allele

Although the patient had compound heterozygous *ZAP70* mutations and reduced expression of ZAP70, there were several different findings from typical ZAP70 deficiency reported previously; i.e. not meeting the criteria of SCID (http://esid.org/Working-Parties/Registry/Diagnosis-criteria) and milder $CD8^+$ T cell lymphopenia. WES revealed the *ZAP70* mutations with 50% of allele frequency (Figure 5A), and ddPCR revealed the X and Y chromosome ratio of 1:1 (Figure 5B), which did not suggest reversion mosaicism or maternal T-cell engraftment. In order to explore

the cause of the hypomorphic phenotype, we hypothesized that a small amount of normal splicing might occur despite the splice site mutation. We cloned PCR products from cDNA spanning exon 3 to 14 of *ZAP70* and analyzed 45 independent clones by Sanger sequencing (Figure 5C). Twenty clones were derived from aberrant splicing without exon 6, and 22 clones had missense mutation (c.1674G>A). The most remarkable result is that 3 clones were derived from normal splicing and did not have missense mutation (c.1674G>A).

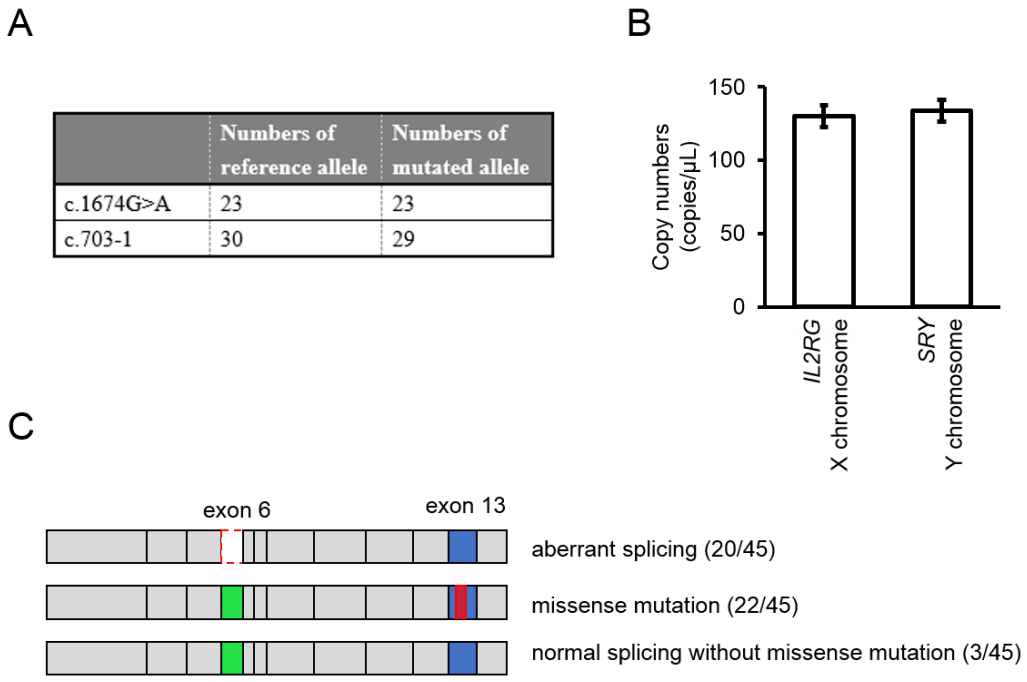

Figure 5. Detection of wild type allele. (A) The numbers of reference allele and mutated allele revealed by whole exome sequencing. (B) The copy numbers of *IL2RG* and *SRY*, which are on X and Y chromosome, respectively, revealed by droplet digital PCR. (C) Schematic representation of the alleles obtained by direct cloning and their numbers.

Assessment of Lymphocyte Function

Signal transduction through the TCR/CD3 complex was examined in each $CD4^+$ or $CD8^+$ T-cell populations. First, TCR-mediated calcium mobilization was analyzed (Figure 6). CD3 cross-linking induced a few and delayed free intracellular Ca^{2+} increases in patient $CD4^+$ and $CD8^+$ T cells. In contrast, ionomycin, which is non-TCR-mediated stimulation, induced free intracellular Ca^{2+} increases to the same degree of the control T cells.

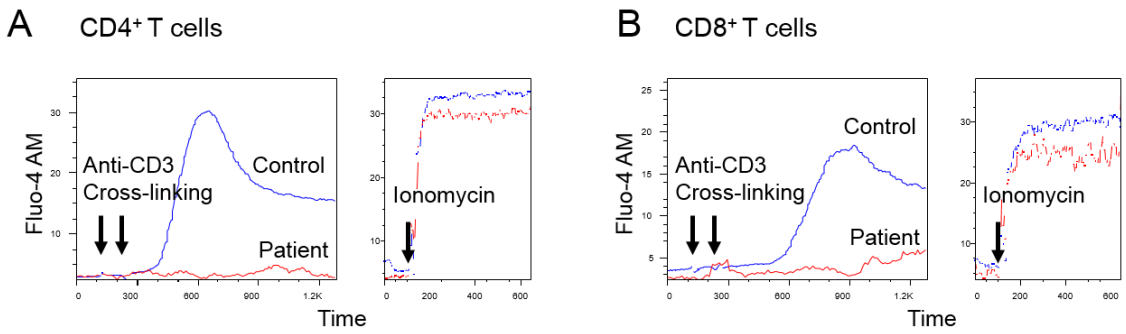

Figure 6. Signal transduction through the TCR/CD3 complex in $CD4^+$ or $CD8^+$ T cells. (A) Calcium mobilization induced by CD3 cross-linking (left) and ionomycin (right) in $CD4^+$ T cells (blue, control; red, patient). (B) Calcium mobilization in $CD8^+$ T cells.

Second, T-cell proliferation after stimulation of the TCR was analyzed (Figure 7). While PMA/ionomycin induced sufficient proliferation of patient T cells, anti-CD3/CD28 induced no proliferation of most T cells and sufficient proliferation of a few but significant T cells, especially $CD4^+$ T cells. These results demonstrates that most T cells are non-functional but a small amount of T cells are normally functional, consisting with the detection of wild type allele.

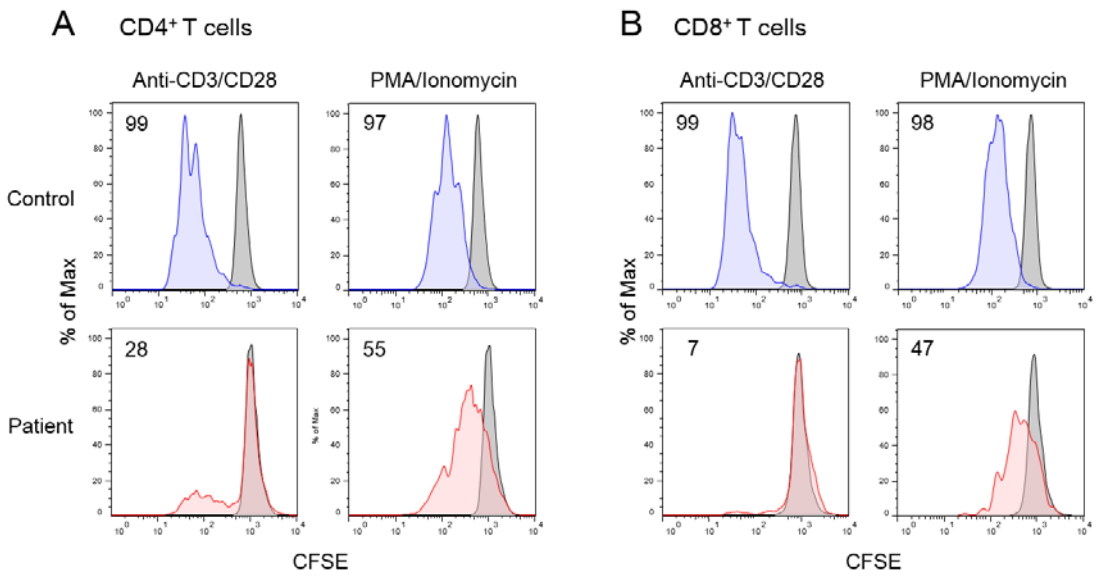

Figure 7. T-cell proliferation analysis in $CD4^+$ or $CD8^+$ T cells. (A) CFSE labeled proliferation induced by anti-CD3/CD28 (left) and PMA/ionomycin (right) in $CD4^+$ T cells. Numbers in plots indicate percent divided cells. (B) CFSE labeled proliferation in $CD8^+$ T cells.

TCR Repertoire

The existence of non-functional T cells made us expect the slight skewing of TCR repertoire as previously described in typical ZAP70 deficiency patients [14]. TCR CDR3 sequences were analyzed using NGS. *TRBV* usage and CDR3 length were slightly skewed (Figure 8A, B, C). Unexpectedly, T cells from the patient had significantly skewed V-J combinations with expansion of *TRBV6-5*/*TRBJ2-7*, *TRBV30*/*TRBJ1-2*, *TRBV18*/*TRBJ2-7* and *TRBV6-6*/*TRBJ2-7* (Figure 9A). The reduced diversity and uneven distribution were observed (Figure 9B, C). Junctional diversity was largely maintained (Figure 8D).

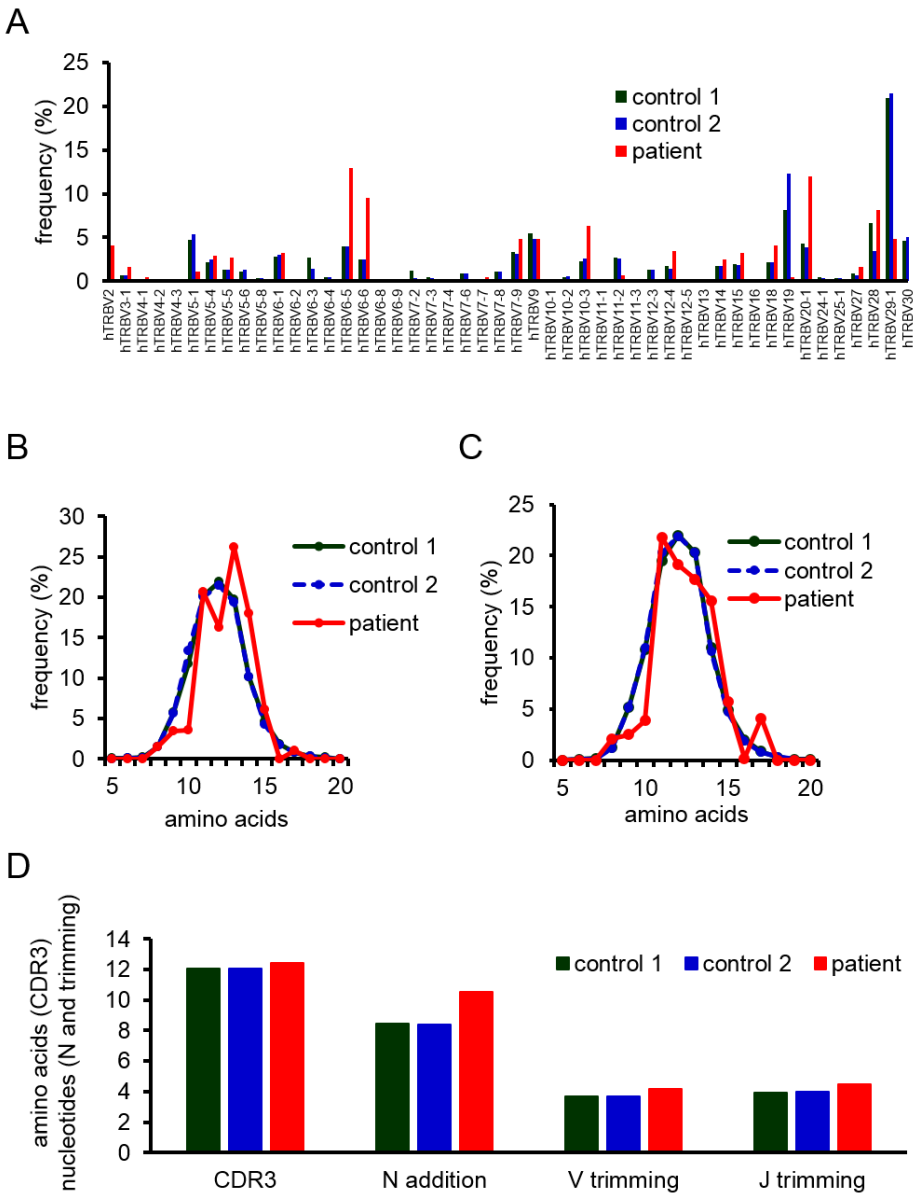

Figure 8. *TRBV* usage, CDR3 length distribution and junctional diversity. (A) The frequency of *TRBV* genes. (B, C) Distribution of CDR3 length frequencies for unique clonotyoes (B) and total clonotypes (C). (D) Mean length of CDR3, N addition, V trimming and J trimming.

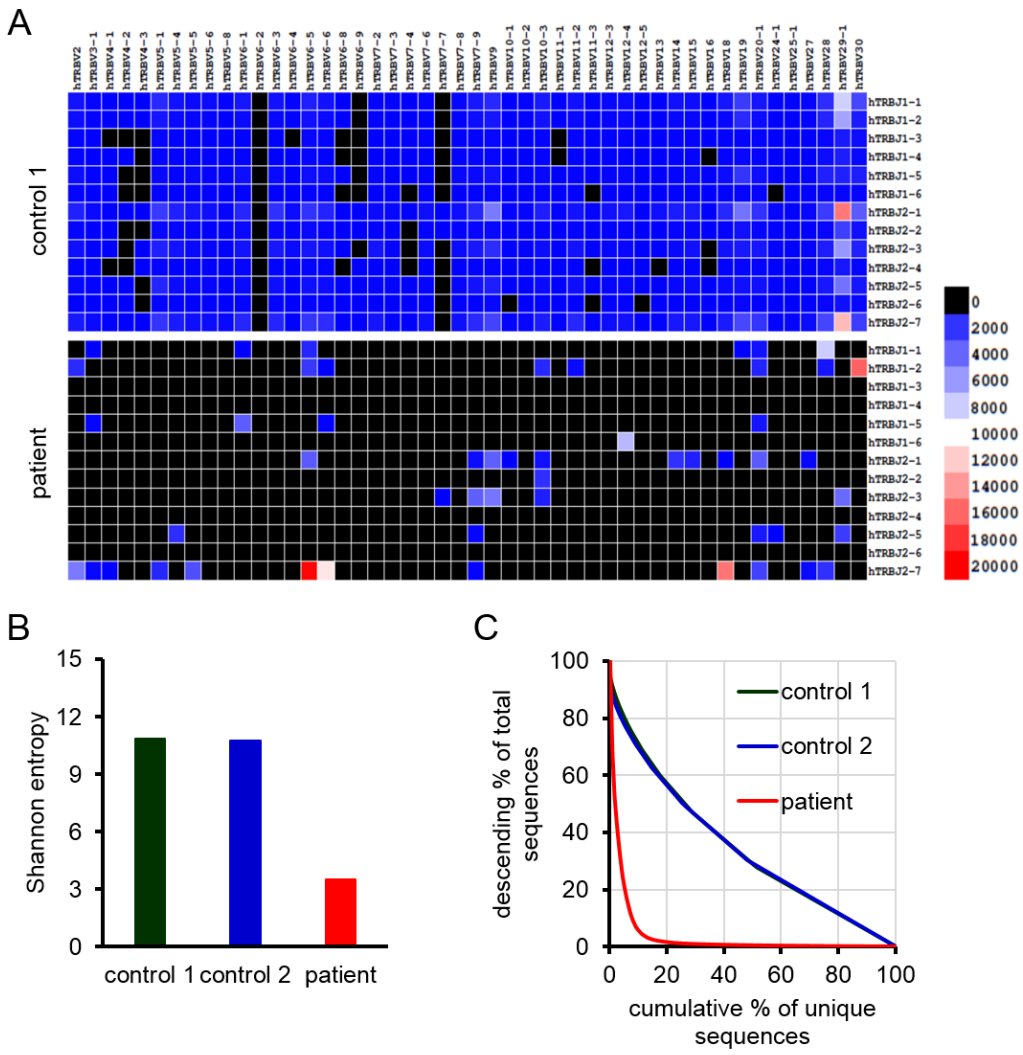

Figure 9. TCR CDR3 sequences. (A) Two-dimensional heat maps of V-J combinations. The relative frequency of *TRBV* is on the x-axis and the relative frequency of *TRBJ* is on the y-axis. (B) Shannon entropy. (C) Graphical presentation of cumulative frequency of unique sequences (x-axis) versus descending frequency of total sequences (y-axis). The slope indicates the degree of the evenness.

Finally, EBV specific *TRBV* CDR3 sequences were investigated (Table 4). Two healthy control subjects had reported clonotypes [32-35]. Of noted, however, the patient had no EBV-

related clonotype despite an extensive literature search although the possibility could not be excluded that unknown EBV-specific sequences were present.

Table 4. EBV specific *TRBV* CDR3 sequence

	EBV specific *TRBV* CDR3 sequence
Control 1	ASSLGNTEAF ASSVGGGTEAF AWSVKGTNTEAF ASSSLNTEAF
Control 2	ASSLGNTEAF ASSVGGGTEAF ASSPSGANVLT ASSPLTDTQY ASSPLAGVGETQY ASSLLAGQETQY
Patient	not detected

EBV, Epstein-Barr virus; CDR3, complementarity determining region 3.

DISCUSSION

We identified a novel hypomorphic mutation of *ZAP70*, and the patient did not manifest SCID but EBV-associated LPD most likely following primary EBV infection. His laboratory manifestations indicated that it was natural to develop EBV-associated LPD.

There are broadly similar laboratory manifestations between our patient and PIDs predisposed to EBV-associated LPD/lymphoma previously described. First, T cells especially naïve T cells are decreased, but not absent, and TCR or associated co-stimulatory signals are impaired. Other T-cell immunodeficiencies present different clinical manifestations. PIDs without T cells most often contract other infectious diseases, which are life-threatening, before EBV infections [36]. Although SCID patients can develop EBV-associated LPD/lymphoma, it is rare as a main feature [37]. PIDs with impaired lymphocyte cytotoxicity, represented by familial

hemophagocytic lymphohistiocytosis (HLH), develop fulminant infectious mononucleosis (FIM) or HLH due to an uncontrolled overwhelming hypercytokinemia produced by activated $CD8^+$ T cells and NK cells [8]. SAP deficiency patients often develop FIM. The reason can be partially explained by the pathology of SAP deficiency including reduced $CD8^+$ T-cell and NK-cell cytotoxicity [8]. ZAP70 plays a pivotal role in TCR signal transduction, which is not directly related to lymphocyte cytotoxicity [12, 13]. In our patient, the development of EBV-associated LPD may have resulted from a limited resistance against the pathogens including live vaccine strains and impaired recognition of EBV-infected cells. Lack of EBV-specific $CD8^+$ T cells and negative titers of EBV antibodies support globally impaired T-cell recognition of EBV antigen. TCR repertoire analysis using NGS confirmed a lack of EBV specific *TRBV* CDR3 sequences at the level of base sequences.

Second, iNKT-cell counts are remarkably decreased. Reduced number of iNKT cells has been reported in SAP deficiency [7, 8], ITK deficiency [9], CD27 deficiency [10], Coronin-1A deficiency [38], and cytidine 5' triphosphate synthase 1 (CTPS1) deficiency [39]. iNKT cells can directly and rapidly recognize EBV-infected cells through CD1d-mediated activation, and mediate direct cytotoxicity, which is especially critical during the earlier stage of EBV infection [40]. iNKT cells are indirectly responsible for controlling EBV infection through NK-cell, T-cell and dendritic-cell activation by the production of IFN-γ and IL-2 [41]. ZAP70 is required for iNKT-cell development during the positive selection, and iNKT cells are absent in *Zap70* null mice [42]. Although the counts of iNKT cells in human ZAP70 deficiency is controversial [3, 43], these findings can help explain the remarkably decreased iNKT-cell counts in the patient.

The third similar manifestations between our patient and PIDs predisposed to EBV-associated LPD/lymphoma is that B-cell counts and development are normal or less impaired.

The majority of EBV-infected cells is B cells, and the presence of B cells is important for EBV-infection [1]. Dysgammaglobulinemia is often observed, but it is result from impaired T-cell function or EBV infection by itself [7-9, 38, 39].

Hypomorphic *ZAP70* mutation resulted in different clinical and laboratory manifestations from those of null mutation. The similar findings has been described in *CORO1A* gene. While loss of function mutations of *CORO1A* are associated with $T^-B^+NK^+$ SCID [44], hypomorphic mutations lead to PID predisposed to EBV-associated LPD/lymphoma [38]. Hypomorphic mutations due to normal splicing have been reported in some diseases [45, 46], including one *ZAP70* patient [47]. The reported patient had had recurrent infections since infancy, and at last in the follow-up, at age 9, he was well without transplantation. Severe EBV infection was not noted, however he developed severe varicella-zoster virus infection. Although the reason of difference of susceptibility to EBV between our patient and the reported patient remains unclear, it may reflect clinical exposure or the impact of genetic defects including iNKT-cell development and TCR signal transduction.

TCR repertoire analysis in great detail using NGS was useful for the evaluation of EBV-specific T cells and T-cell development. This analysis is superior to the previous antigen-specific T-cell analysis such as major histocompatibility complex-peptide tetramer staining, enzyme-linked immunospot assay, or intracellular cytokine assay in the evaluation of the variety and amount. Furthermore, it can be comprehensively analyzed in 1 NGS run. If more antigen-specific CDR3 sequences are known, this new method will be applied to the other infection or autoimmunity. Significant restriction of the TCR repertoire with reduced diversity and uneven distribution in ZAP70-deficient patient likely indicate the abnormal T-cell generation and the nonrandom usage of V, D and J elements, which may contribute to the selective susceptibility to

EBV infection. Abnormality of central and peripheral tolerance may also be involved [25]. These results confirm and extend previous findings of ZAP70 involvement at the immature single positive thymocyte stage to the double positive thymocyte stage [14].

ZAP70 alterations have a wide spectrum of clinical features. While loss of function mutations of *ZAP70* lead to SCID [12], hypomorphic mutations of *ZAP70* seem to be associated with the autoimmune disease [48, 49]. We identified a novel hypomorphic mutation of *ZAP70* and described a selective dysregulation of EBV infection. Our findings extend the spectrum of clinical features of *ZAP70* alterations, and indicated pivotal roles of T-cell recognition and iNKT cells in immune response against EBV (Figure 10).

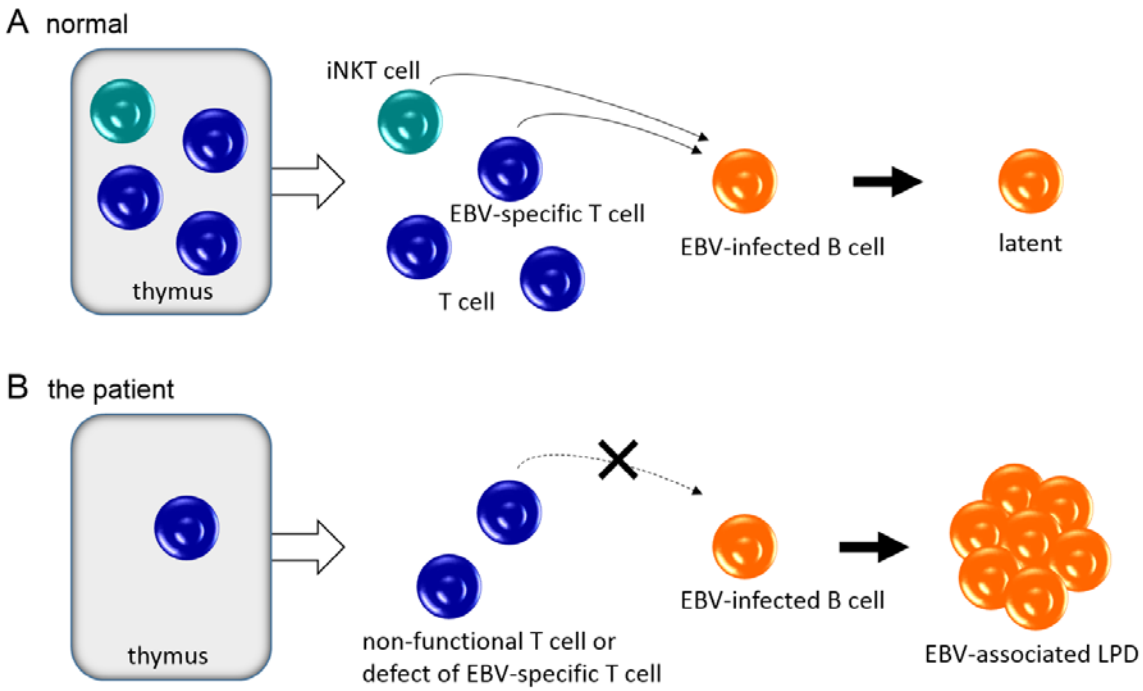

Figure 10. Schematic representation of the invariant natural killer (iNKT)-cell and T-cell development and regulation of EBV infection. (A) iNKT cells (green) and T cells (blue) migrate to the periphery after development in the thymus. EBV-infected B cells (orange)

are controlled by normal immune response including iNKT cells and EBV-specific T cells. (B) The *ZAP70*-mutated patient has impairment of iNKT-cell and EBV-specific T-cell development in the thymus. The T cells in the periphery are non-functional or not EBV-specific. EBV-infected B cells result in LPD.

Appendix: Supplementary data

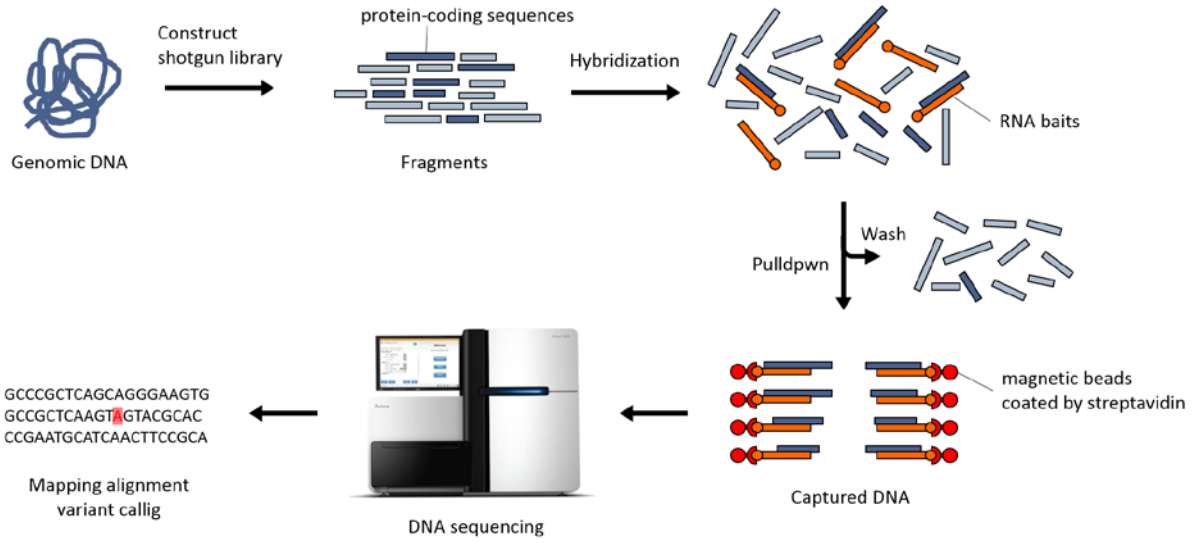

Supplementary Figure 1. Workflow for whole exome sequencing (modified from reference 15). Genomic DNA is randomly sheared, and the library fragments are flanked by adaptors (not shown). The fragments are hybridized to biotinylated RNA baits (orange), which bind to protein-coding sequences (dark blue). Recovery of the hybridized fragments by biotin-streptavidin-based pulldown is followed by amplification and massively parallel sequencing of the enriched, amplified library and the mapping and calling of candidate causal variants.

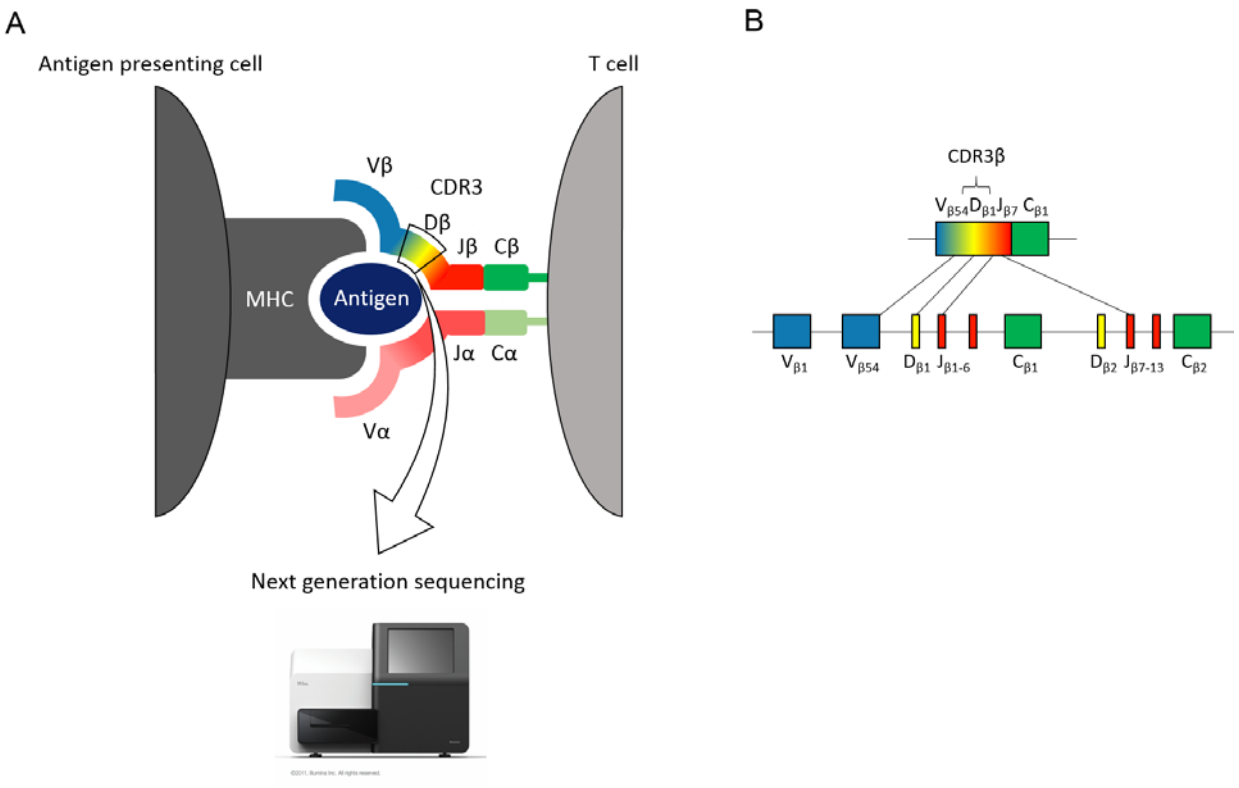

Supplementary Figure 2. TCR-antigen-MHC interaction and TCR gene recombination (modified from reference 24). (A) The antigen presenting cell (APC) presents peptide antigen in complex with the major histocompatibility complex (MHC), and the T-cell receptor (TCR) binds to both the antigen and MHC. The TCR consists of an α and β chain, which include the constant region (green), the J region (red), the D region (yellow) and the V region (blue). The TCR α chain does not have the D region. The complementarity determining region 3 (CDR3) domain (multi-colored), approximately 45 nucleotides long, comprises the VJ (for TCR-α) or VDJ (for TCR-β) junction. The CDR3 regions are the main domains which contact with peptide antigen, and largely determine TCR specificity. (B) Schematic representation of TCR-β VDJ gene recombination. Initially one of the two D regions is joined with one of 13 J regions, followed by joining of the DJ region to one of more than 50 V regions, yielding a final VDJ region. This mechanism contributes the variety and diversity of the TCR.

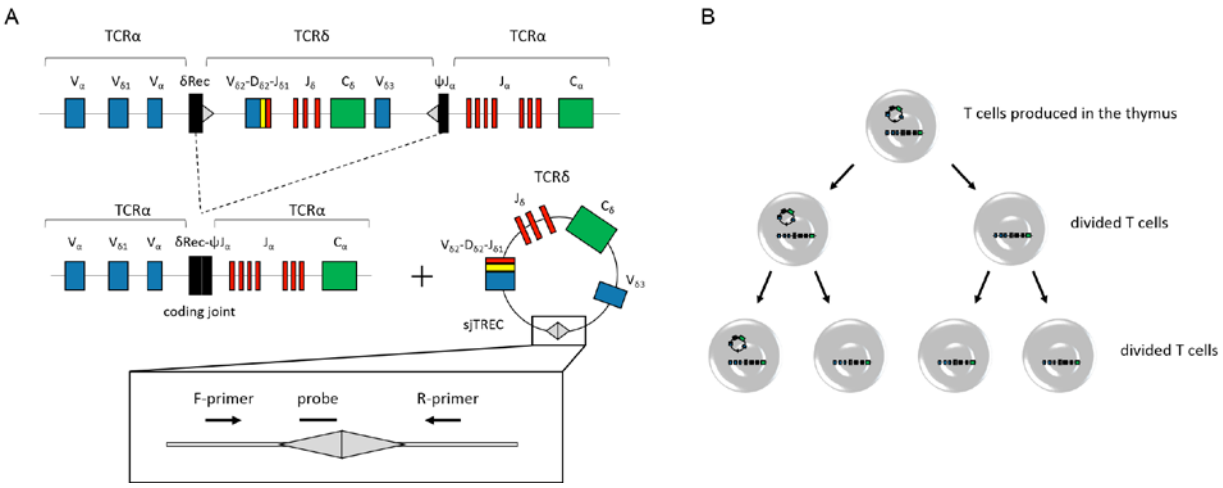

Supplementary Figure 3. Generation of T-cell receptor excision circles (TRECs) and T-cell division. (A) *TCRD*, which codes for the T-cell receptor (TCR)-δ, are embedded in *TCRA* codes for the TCR-α. For the formation of the TCR-α, *TCRD* is excised and ligated, result in a small circular DNA fragment with a characteristic signal joint DNA region. Because the sequences of the ligated region are specific, they can be quantified by real-time PCR using specific primers (arrows). (B) TRECs do not multiply during cell division. Therefore, TRECs quantification is useful for determining recent thymic emigrants [26].

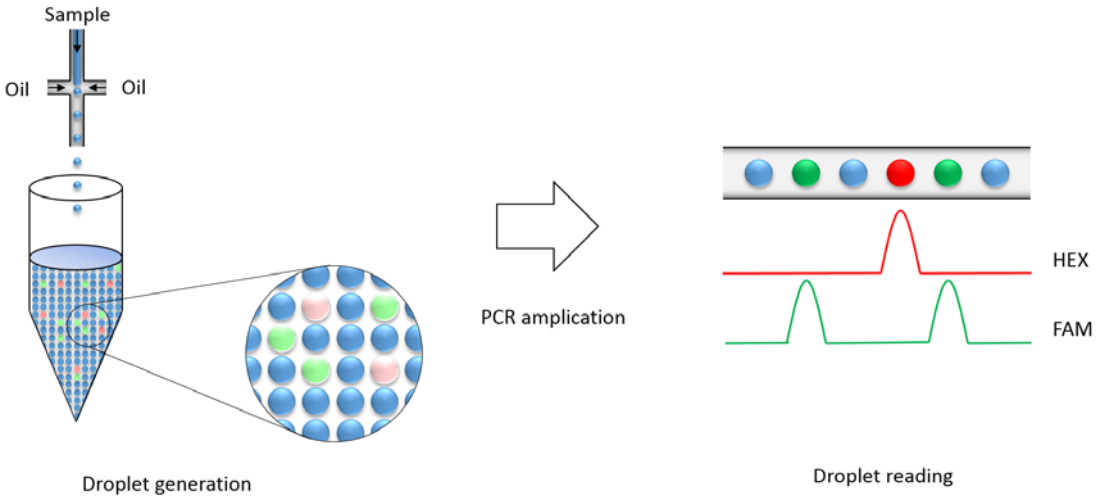

Supplementary Figure 4. Droplet digital PCR. Samples are partitioned into 20,000 nanoliter-sized droplets. Target (light red) and background (light green) DNA are randomly distributed into the droplets. Droplets having neither target nor background DNA are indicated in blue. Following PCR amplification with conventional TaqMan assays using the primers and the hydrolysis probes labeled with HEX or FAM, each droplets are individually analyzed. Red and blue droplets show droplets contain amplified target or background DNA, respectively. This system can quantify the nucleic acid in the sample with accuracy [28].

Supplementary Table 1: Primers information

	Forward primers (5' to 3')	Reverse primers (5' to 3')
genomic DNA, exon 6	TGGGAAGACGGTGTACCACT	GAGCAGAAGGGACAGTGAGG
genomic DNA, exon 13	CTACGGCCAGAAGCCCTAC	AACCCTGGTGTGTTGGAGAG
cDNA, exon 5-10	TGGGAAGACGGTGTACCACT	CTCTTCCGTGTCTGCCTTCT
cDNA, exon 3-14	CACTGTGGACCGGCAGAG	GCTGGCCAGGCTGTAGTAAC

Supplementary Table 2: Monoclonal antibodies information

Specificity	Conjugation	Clone	Manufacture
CD3	VioGreen	BW264/56	Miltenyi Biotec
CD4	VioBlue	M-T466	Miltenyi Biotec
CD8	PE-Vio770	BW135/80	Miltenyi Biotec
CD16	FITC	3G8	Beckman Coulter
CD19	VioBlue	LT19	Miltenyi Biotec
CD20	VioGreen	LT20	Miltenyi Biotec
CD25	PC5	B1.49.9	Beckman Coulter
CD31	APC	AC128	Miltenyi Biotec
CD45RA	ECD	2H4LDH11LDB9	Beckman Coulter
CD45RO	APC-Vio770	UCHL1	Miltenyi Biotec
CD56	PC5	N901 (NKH-1)	Beckman Coulter
CD62L	PC5	DREG56	Beckman Coulter
CD127	APC	MB15-18C9	Miltenyi Biotec
CD185	PerCP/Cy5.5	J252D4	BioLegend
CD194	PE/Cy7	L291H4	BioLegend
CD197	Alexa Fluor 700	150503	BD Pharmingen
TCRαβ	PE	BW242/412	Miltenyi Biotec
TCRγδ	FITC	11F2	Miltenyi Biotec
TCR Vα24	FITC	C15	Beckman Coulter
TCR Vβ11	PE	C21	Beckman Coulter

Supplementary Table 3: Primers and probes information for droplet digital PCR

	Forward primers (5' to 3')	Reverse primers (5' to 3')	Probes
IL2RG	ACTCCCTCAGTGTTTCC	TACTCGACATTGAACACAAA	CCTCTGGGAGGGGC
SRY	CTAGGTAGGTCTTTGTA	CACACACTCAAGAATG	CCGATTGTCCTACAGC

References

1. Rickinson AB, Long HM, Palendira U, Münz C, Hislop AD. Cellular immune controls over Epstein-Barr virus infection: new lessons from the clinic and the laboratory. Trends Immunol 2014; 35: 159-69.
2. Parvaneh N, Filipovich AH, Borkhardt A. Primary immunodeficiencies predisposed to Epstein-Barr virus-driven haematological diseases. Br J Haematol 2013; 162: 573-86.
3. Palendira U, Rickinson AB. Primary immunodeficiencies and the control of Epstein-Barr virus infection. Ann N Y Acad Sci 2015. [Epub ahead of print]
4. Petrara MR, Freguja R, Gianesin K, Zanchetta M, De Rossi A. Epstein-Barr virus-driven lymphomagenesis in the context of human immunodeficiency virus type 1 infection. Front Microbiol 2013; 4: 311.
5. Nourse JP, Jones K, Gandhi MK. Epstein-Barr Virus-related post-transplant lymphoproliferative disorders: pathogenetic insights for targeted therapy. Am J Transplant 2011; 11: 888-95.
6. Chijioke O, Müller A, Feederle R, et al. Human natural killer cells prevent infectious mononucleosis features by targeting lytic Epstein-Barr virus infection. Cell Rep 2013; 5: 1489-98.
7. Booth C, Gilmour KC, Veys P, et al. X-linked lymphoproliferative disease due to SAP/SH2D1A deficiency: a multicenter study on the manifestations, management and outcome of the disease. Blood 2011; 117: 53-62.
8. Yang X, Miyawaki T, Kanegane H. SAP and XIAP deficiency in hemophagocytic lymphohistiocytosis. Pediatr Int 2012; 54: 447-54.
9. Ghosh S, Bienemann K, Boztug K, Borkhardt A. Interleukin-2-inducible T-cell kinase (ITK)

deficiency - clinical and molecular aspects. J Clin Immunol 2014; 34: 892-9.

10. van Montfrans JM, Hoepelman AI, Otto S, et al. CD27 deficiency is associated with combined immunodeficiency and persistent symptomatic EBV viremia. J Allergy Clin Immunol 2012; 129: 787-93.
11. Li FY, Chaigne-Delalande B, Su H, Uzel G, Matthews H, Lenardo MJ. XMEN disease: a new primary immunodeficiency affecting Mg2+ regulation of immunity against Epstein-Barr virus. Blood 2014; 123: 2148-52.
12. Fischer A, Picard C, Chemin K, Dogniaux S, le Deist F, Hivroz C. ZAP70: a master regulator of adaptive immunity. Semin Immunopathol 2010; 32: 107-16.
13. Wang H, Kadlecek TA, Au-Yeung BB, et al. ZAP-70: an essential kinase in T-cell signaling. Cold Spring Harb Perspect Biol 2010; 2: a002279.
14. Roifman CM, Dadi H, Somech R, Nahum A, Sharfe N. Characterization of ζ-associated protein, 70 kd (ZAP70)-deficient human lymphocytes. J Allergy Clin Immunol 2010; 126: 1226-33.
15. Bamshad MJ, Ng SB, Bigham AW, et al. Exome sequencing as a tool for Mendelian disease gene discovery. Nat Rev Genet 2011; 12: 745-55.
16. Kunishima S, Okuno Y, Yoshida K, et al. ACTN1 mutations cause congenital macrothrombocytopenia. Am J Hum Genet. 2013; 92: 431-8.
17. Li H, Durbin R. Fast and accurate short read alignment with Burrows-Wheeler transform. Bioinformatics 2010; 26: 589-95.
18. Li H, Handsaker B, Wysoker A, et al. The Sequence Alignment/Map format and SAMtools. Bioinformatics 2009; 25: 2078-9.
19. Wang K, Li M, Hakonarson H. ANNOVAR: functional annotation of genetic variants from

high-throughput sequencing data. Nucleic Acids Res 2010; 38: e164.

20. Kumar P, Henikoff S, Ng PC. Predicting the effects of coding non-synonymous variants on protein function using the SIFT algorithm. Nat Protoc 2009; 4: 1073-81.
21. Pollard KS, Hubisz MJ, Rosenbloom KR, Siepel A. Detection of nonneutral substitution rates on mammalian phylogenies. Genome Res 2010; 20: 110-21.
22. Adzhubei IA, Schmidt S, Peshkin L, et al. A method and server for predicting damaging missense mutations. Nat Methods 2010; 7: 248-9.
23. Schwarz JM, Rödelsperger C, Schuelke M, Seelow D. MutationTaster evaluates disease-causing potential of sequence alterations. Nat Methods 2010; 7: 575-6.
24. Woodsworth DJ, Castellarin M, Holt RA. Sequence analysis of T-cell repertoires in health and disease. Genome Med 2013; 5: 98
25. Yu X, Almeida JR, Darko S, et al. Human syndromes of immunodeficiency and dysregulation are characterized by distinct defects in T-cell receptor repertoire development. J Allergy Clin Immunol 2014; 133: 1109-15.
26. Hazenberg MD, Verschuren MC, Hamann D, Miedema F, van Dongen JJ. T cell receptor excision circles as markers for recent thymic emigrants: basic aspects, technical approach, and guidelines for interpretation. J Mol Med (Berl) 2001; 79: 631-40.
27. Morinishi Y, Imai K, Nakagawa N, et al. Identification of severe combined immunodeficiency by T-cell receptor excision circles quantification using neonatal guthrie cards. J Pediatr 2009; 155: 829-33.
28. Hindson BJ, Ness KD, Masquelier DA, et al. High-throughput droplet digital PCR system for absolute quantitation of DNA copy number. Anal Chem 2011; 83: 8604-10.
29. Stiehm ER, Fudenberg HH. Serum levels of immune globulins in health and disease: a survey.

Pediatrics 1966; 37: 715-27.

30. Ok CY, Li L, Young KH. EBV-driven B-cell lymphoproliferative disorders: from biology, classification and differential diagnosis to clinical management. Exp Mol Med 2015; 47: e132.
31. Pettersen EF, Goddard TD, Huang CC, et al. UCSF Chimera--a visualization system for exploratory research and analysis. J Comput Chem 2004; 25: 1605-12.
32. Miconnet I, Marrau A, Farina A, et al. Large TCR diversity of virus-specific CD8 T cells provides the mechanistic basis for massive TCR renewal after antigen exposure. J Immunol 2011; 186: 7039-49.
33. Iancu EM, Corthesy P, Baumgaertner P, et al. Clonotype selection and composition of human CD8 T cells specific for persistent herpes viruses varies with differentiation but is stable over time. J Immunol 2009; 183: 319-31.
34. Venturi V, Chin HY, Asher TE, et al. TCR beta-chain sharing in human CD8+ T cell responses to cytomegalovirus and EBV. J Immunol 2008; 181: 7853-62.
35. Price DA, Brenchley JM, Ruff LE, et al. Avidity for antigen shapes clonal dominance in CD8+ T cell populations specific for persistent DNA viruses. J Exp Med 2005; 202: 1349-61.
36. Notarangelo LD. Primary immunodeficiencies. J Allergy Clin Immunol 2010; 125 (2 Suppl 2): S182-94.
37. Newell A, Dadi H, Goldberg R, Ngan BY, Grunebaum E, Roifman CM. Diffuse large B-cell lymphoma as presenting feature of Zap-70 deficiency. J Allergy Clin Immunol 2011; 127: 517-20.
38. Moshous D, Martin E, Carpentier W, et al. Whole-exome sequencing identifies Coronin-1A deficiency in 3 siblings with immunodeficiency and EBV-associated B-cell

lymphoproliferation. J Allergy Clin Immunol 2013; 131: 1594-603.

39. Martin E, Palmic N, Sanquer S, et al. CTP synthase 1 deficiency in humans reveals its central role in lymphocyte proliferation. Nature 2014; 510: 288-92.
40. Chung BK, Tsai K, Allan LL, et al. Innate immune control of EBV-infected B cells by invariant natural killer T cells. Blood 2013; 122: 2600-8.
41. Priatel JJ, Chung BK, Tsai K, Tan R. Natural killer T cell strategies to combat Epstein-Barr virus infection. Oncoimmunology 2014; 3: e28329.
42. Iwabuchi K, Iwabuchi C, Tone S, et al. Defective development of NK1.1+ T-cell antigen receptor alphabeta+ cells in zeta-associated protein 70 null mice with an accumulation of NK1.1+ CD3- NK-like cells in the thymus. Blood 2001; 97: 1765-75.
43. Hauck F, Blumenthal B, Fuchs S, Lenoir C, Martin E, Speckmann C, et al. SYK expression endows human ZAP70-deficient CD8 T cells with residual TCR signaling. Clin Immunol 2015; 161: 103-9.
44. Shiow LR, Roadcap DW, Paris K, et al. The actin regulator coronin 1A is mutant in a thymic egress-deficient mouse strain and in a patient with severe combined immunodeficiency. Nat Immunol 2008; 9: 1307-15.
45. Karakawa S, Okada S, Tsumura M, et al. Decreased expression in nuclear factor-κB essential modulator due to a novel splice-site mutation causes X-linked ectodermal dysplasia with immunodeficiency. J Clin Immunol 2011; 31: 762-72.
46. Sobacchi C, Pangrazio A, Lopez AG, et al. As little as needed: the extraordinary case of a mild recessive osteopetrosis owing to a novel splicing hypomorphic mutation in the TCIRG1 gene. J Bone Miner Res 2014; 29: 1646-50.
47. Picard C, Dogniaux S, Chemin K, et al. Hypomorphic mutation of ZAP70 in human results

in a late onset immunodeficiency and no autoimmunity. Eur J Immunol 2009; 39: 1966-76.

48. Turul T, Tezcan I, Artac H, et al. Clinical heterogeneity can hamper the diagnosis of patients with ZAP70 deficiency. Eur J Pediatr 2009; 168: 87-93.
49. Haluk Akar H, Patiroglu T, Akyildiz BN, et al. Silent brain infarcts in two patients with zeta chain-associated protein 70kDa (ZAP70) deficiency. Clin Immunol 2015; 158: 88-91.

Publications

1. Fuke T, Abe Y, Hoshino A, Oto H, Sakai N, Murayama J, Yoshida K, Itabashi K. [Cefazolin efficacy and antibiotic sensitivity against pathogenic bacteria in pediatric with acute upper urinary tract infection]. Kansenshogaku Zasshi 2010; 84: 269-75. Japanese.
2. Hibino S, Fukuchi K, Abe Y, Hoshino A, Sakurai S, Mikawa T, Fuke T, Yoshida K, Itabashi K. [Four infants with upper urinary tract infection due to extended-spectrum bata lactamase (ESBL)-producing Escherichia coli]. Kansenshogaku Zasshi 2011; 85:481-7. Japanese.
3. Nomura K, Hoshino A, Miyawaki T, Hama A, Kojima S, Kanegane H. Neutropenia and myeloid dysplasia in a patient with delayed-onset adenosine deaminase deficiency. Pediatr Blood Cancer 2013; 60: 885-6.
4. Hoshino A, Fujii T, Hibino S, Abe Y, Onda H, Itabashi K. Acute infantile dacryoadenitis. J Pediatr 2014; 164: 425. e1.
5. Hibino S, Hoshino A, Fujii T, Abe Y, Watanabe S, Uemura O, Itabashi K. Post-streptococcal acute glomerulonephritis associated with pneumococcal infection. Pediatr Int 2013; 55: e136-8.
6. Hoshino A, Shimizu M, Matsukura H, Sakaki-Nakatsubo H, Nomura K, Miyawaki T, Kanegane H. Allogeneic bone marrow transplantation appears to ameliorate IgA nephropathy in a patient with X-linked thrombocytopenia. J Clin Immunol 2014; 34: 53-7.
7. Hoshino A, Imai K, Ohshima Y, Yasutomi M, Kasai M, Terai M, Ishigaki K, Morio T, Miyawaki T, Kanegane H. Pneumothorax in patients with severe combined immunodeficiency. Pediatr Int 2014; 56:510-4.
8. Hoshino A, Nomura K, Noguchi K, Kanegane H. Relapsed leukemia without peripheral blood abnormalities and clinical symptoms detected on MRI. Pediatr Int 2014; 56: 798.

9. Hoshino A, Nomura K, Hamashima T, Isobe T, Seki M, Hiwatari M, Yoshida K, Shiraishi Y, Chiba K, Tanaka H, Miyano S, Ogawa S, Takita J, Kanegane H. Aggressive transformation of anaplastic large cell lymphoma with increased number of ALK-translocated chromosomes. Int J Hematol 2015; 101: 198-202.
10. Hoshino A, Okuno Y, Migita M, Ban H, Yang X, Kiyokawa N, Adachi Y, Kojima S, Ohara O, Kanegane H. X-linked agammaglobulinemia associated with B-precursor acute lymphoblastic leukemia. J Clin Immunol 2015; 35: 108-11.
11. Yang X, Hoshino A, Taga T, Kunitsu T, Ikeda Y, Yasumi T, Yoshida K, Wada T, Miyake K, Kubota T, Okuno Y, Muramatsu H, Adachi Y, Miyano S, Ogawa S, Kojima S, Kanegane H. A female patient with incomplete hemophagocytic lymphohistiocytosis caused by a heterozygous XIAP mutation associated with non-random X-chromosome inactivation skewed towards the wild-type XIAP allele. J Clin Immunol 2015; 35: 244-8.
12. Kawasaki Y, Makimoto M, Nomura K, Hoshino A, Hamashima T, Hiwatari M, Nakazawa A, Takita J, Yoshida T, Kanegane H. Neonatal acute megakaryoblastic leukemia mimicking congenital neuroblastoma. Clin Case Rep 2015; 3: 145-9.
13. Okuno Y, Hoshino A, Muramatsu H, Kawashima N, Wang X, Yoshida K, Wada T, Gunji M, Toma T, Kato T, Shiraishi Y, Iwata A, Hori T, Kitoh T, Chiba K, Tanaka H, Sanada M, Takahashi Y, Nonoyama S, Ito M, Miyano S, Ogawa S, Kojima S, Kanegane H. Late-onset combined immunodeficiency with a novel *IL2RG* mutation and probable revertant somatic mosaicism. J Clin Immunol 2015 Sep 26. [Epub ahead of print].
14. Hoshino A, Takashima T, Yoshida K, Morimoto A, Kawahara Y, Yeh TW, Okano T, Yamashita M, Mitsuiki N, Imai K, Sakatani T, Nakazawa A, Okuno Y, Shiraishi Y, Chiba K, Tanaka H, Miyano S, Ogawa S, Kojima S, Morio T, Kanegane H. Selective dysregulation of

Epstein-Barr virus infection in hypomorphic *ZAP70* mutation. (submitted).